Inorg. Chem. **2006**, *45*, 9114–9122

Syntheses, Crystal Structures, and Magnetic Properties of $[Ln^{III}_2(Succinate)_3(H_2O)_2]\cdot 0.5H_2O$ [Ln = Pr, Nd, Sm, Eu, Gd, and Dy] Polymeric Networks: Unusual Ferromagnetic Coupling in Gd Derivative

Subal Chandra Manna,[†] Ennio Zangrando,[‡] Alessandro Bencini,*[,§] Cristiano Benelli,[§] and Nirmalendu Ray Chaudhuri*[,†]

Department of Inorganic Chemistry, Indian Association for the Cultivation of Science, Kolkata-7000 32, Dipartimento di Scienze Chimiche, University of Trieste, 34127 Trieste, Italy, and Dipartimento di Chimica, Università di Firenze, Polo Scientifico di Sesto Fiorentino, 50019 Sesto Fiorentino (FI), Italy

Received May 11, 2006

Lanthanide-organic coordination polymeric networks of $[Ln^{III}_2(suc)_3(H_2O)_2]\cdot 0.5H_2O$ [suc = succinate dianion, Ln = Pr (**1**), Nd (**2**), Sm (**3**), Eu (**4**), Gd (**5**), and Dy (**6**)] have been synthesized and characterized by single-crystal X-ray diffraction analyses. The structural determination reveals that complexes are isomorphous, all crystallizing in monoclinic system, space group *I*2/a. The complexes possess a 3D architecture with Ln ion in a nine-coordination geometry attained by eight oxygen atoms from succinate and one oxygen atom from an aqua ligand. Low-temperature magnetic study indicates that ferromagnetic interaction is present in case of Gd(III) and Dy(III). Antiferromagnetic interaction is observed for the rest of the complexes. Density functional theory calculations are performed which support the existence of a superexchange ferromagnetic coupling in Gd(III) ions, whereas classical crystal field model has been applied to study the complexes **1**, **2**, **3**, and **6**.

Introduction

Coordination polymers of rare-earth metals have received significant attention in the current research because of their wide range of application such as magnetic material,[1] liquid crystals,[2] luminescent sensors and light converters,[3,4] molecular-recognition and chirality-sensing agents in biology,[5] DNA hydrolysis promoters,[6] shift reagent in NMR spectroscopy,[7] tags for time-resolved luminescence microscopy,[8] magnetic alloys for refrigeration,[9] precursors for superconducting materials,[10] MRI contrast agents,[11] and reagents in

* To whom correspondence should be addressed. E-mail: icnrc@iacs.res.in (N.R.C.), alessandro.bencini@unifi.it (A.B.).
[†] Indian Association for the Cultivation of Science.
[‡] University of Trieste.
[§] Universitá di Firenze

(1) (a) Sanada, T.; Suzuki, T.; Yoshida, T.; Kaizaki, S. *Inorg. Chem.* **1998**, *37*, 4712. (b) Decurtins, S.; Gross, M.; Schmalle, H. W.; Ferlay, S. *Inorg. Chem.* **1998**, *37*, 2443. (c) Costes, J. P.; Dupuis, A.; Laurent, J. P. *J. Chem. Soc., Dalton Trans.* **1998**, 735. (d) Winpenny, R. E. P. *Chem. Soc. Rev.* **1998**, *27*, 447. (e) Costes, J. P.; Dahan, F.; Dupuis, A.; Laurent, J. P. *Inorg. Chem.* **1997**, *36*, 3429. (f) Ramade, I.; Kahn, O.; Jeannin, Y.; Robert, F. *Inorg. Chem.* **1997**, *36*, 930. (g) Sanz, J. L.; Ruiz, R.; Gleizes, A.; Lloret, F.; Faus, J.; Julve, M.; Borrás-Almenar, J. J.; Journaux, Y. *Inorg. Chem.* **1996**, *35*, 7384. (h) Benelli, C.; Caneschi, A.; Gatteschi, D.; Sessoli, R. *J. Appl. Phys.* **1993**, *73*, 5333. (i) Benelli, C.; Caneschi, A.; Gatteschi, D.; Sessoli, R. *Inorg. Chem.* **1993**, *32*, 4797. (j) Benelli, C.; Caneschi, A.; Gatteschi, D.; Pardi, L.; Rey, P. *Inorg. Chem.* **1990**, *29*, 4223. (k) Benelli, C.; Caneschi, A.; Gatteschi, D.; Pardi, L.; Rey, P.; Shum, D. P.; Carlin, R. L. *Inorg. Chem.* **1989**, *28*, 272. (l) Benelli, C.; Caneschi, A.; Gatteschi, D.; Pardi, L.; Rey, P. *Inorg. Chem.* **1989**, *28*, 275. (m) Setyiawati, A.; Liu, S.; Rettig, S. J.; Thomson, R. C.; Orvig, C. *Inorg. Chem.* **2000**, *39*, 496.
(2) Binnemans, K.; Gorller-Walrand, C. *Chem. Rev.* **2002**, *102*, 2303.
(3) Sabbatini, N.; Guardigli, M.; Lehn, J. M. *Coord. Chem. Rev.* **1993**, *123*, 201.
(4) Kido, J.; Okamoto, Y. *Chem. Rev.* **2002**, *102*, 2357.
(5) Tsukube, H.; Shinoda, S. *Chem. Rev.* **2002**, *102*, 2389.
(6) Liu, C.; Wang, M.; Zhang, T.; Sun, H. *Coord. Chem. Rev.* **2004**, *248*, 147.
(7) (a) Cockerill, A. F.; Davies, G. L. O.; Harden, R. C.; Rackham, D. M. *Chem. Rev.* **1973**, *73*, 553. (b) Mayo, B. C. *Chem. Soc. Rev.* **1973**, *2*, 49. (c) Sink, R. M.; Buster, D. C.; Sherry, A. D. *Inorg. Chem.* **1990**, *29*, 3645. (d) Buster, D. C.; Castro, M. M. C. A.; Geraldes, C. F. G. C.; Malloy, C. R.; Sherry, A. D.; Siemers, T. C. *Magn. Reson. Med.* **1990**, *15*, 25. (e) Bansal, N.; Germann, M. J.; Lazar, I.; Malloy, C. R.; Sherry, A. D. *J. Magn. Reson. Imaging* **1992**, *2*, 385.
(8) Charbonnie're, L. J.; Ziessel, R.; Guardigli, M.; Roda, A.; Sabbatini, N.; Cesario, M. *J. Am. Chem. Soc.* **2001**, *123*, 2436 and references therein.
(9) (a) Pecharsky, V. K. L.; Gschneidner, K. A., Jr. *J. Magn. Magn. Mater.* **1999**, *200*, 44. (b) Gschneidner, K. A., Jr.; Pecharsky, V. K. L. *J. Appl. Phys.* **1999**, *85*, 5365.
(10) (a) Hubert-Pfalzgraf, L. G. *New J. Chem.* **1995**, *19*, 727. (b) Gleizes, A.; Julve, M.; Kuzmina, N.; Alikhanyan, A.; Lloret, F.; Malkerova, I.; Sanz, J. L.; Senocq, F. *Eur. J. Inorg. Chem.* **1998**, 1169.

10.1021/ic060807d CCC: $33.50
Published on Web 09/29/2006

organic synthesis and catalysis.[12,13] Literature survey shows that reports of lanthanide coordination frameworks dealing with magnetic properties are scarce in comparison to transition metals. This is attributed to the simplified spin Hamiltonian approach, useful in understanding and parametrizing the magnetic interaction in case of d^n metal ions but is not applicable in lanthanide systems for the presence of large unquenched orbital angular momentum.[14] The presence of this large unquenched orbital momentum generates magnetic anisotropy which is required for magnetically ordered materials with large coercive fields.[14,15]

Moreover, since the magnetic interactions involved in the f electron pairs are weak, and sometimes masked by the crystal field effects on the magnetic susceptibility, the analysis of the experimental data becomes more difficult,[14] and no simple models are available for the qualitative interpretation and rational analysis of the magnetic properties of lanthanide analogues to those developed for transition-metal ions.[16−18] Thus researchers, attracted in exploring lanthanide ions in the field of molecule-based magnetic materials, are facing extreme difficulty in the interpretation of magnetic properties because of the lack of qualitative models. However, for the gadolinium(III) (f^7) system, which has no orbital momentum, some publications describing the structural network as well as magnetic properties have been recently reported.[19−21] Generally, the interaction between the adjacent gadolinium ions is antiferromagnetic in nature and the extent of antiferromagnetism lies in the range $0.045 \leq |J| \leq 0.21\ cm^{-1}$.[20] To the best of our knowledge, only a few gadolinium-containing networks are reported to date showing ferromagnetic interactions[21] and, in all cases, carboxylates are used as building blocks, for example, 3D malonato-bridged Gd(III) complex reported by Hernández-Molina et al.,[21b] except in the very recent complex with dinitrogen as the bridging group,[21e] where some magneto-structural correlations based on density functional theory (DFT) calculation are presented.

As a matter of fact, a few papers of succinato-bridged lanthanide (Sc, Y, La, Pr, Gd, Er, and Lu[22,23]) networks report only the synthesis and structural characterization and are devoid of low-temperature magnetic study. These observations have prompted us to synthesize and evaluate magnetic interactions in the lanthanide carboxylate system by using the flexible succinate dianion, which possesses the ability to form architecture with metal ions of diverse size and shape adopting different coordination modes.[24] The Present Contribution reports syntheses and crystal structures of $[Ln^{III}_2(suc)_3(H_2O)_2]\cdot 0.5H_2O$ [suc = succinate dianion, Ln = Pr (**1**), Nd (**2**), Sm (**3**), Eu (**4**), Gd (**5**), and Dy (**6**)] along with the low-temperature magnetic studies of **1**, **2**, **3**, **5**, and **6**. DFT calculations have been performed on the Gd(III) complex to clarify the nature and the extent of the magnetic interactions. These calculations furnish also the theoretical support in interpreting the observed magnetic data.

Experimental Section

Materials. High purities of gadolinium nitrate hexahydrate, praseodymium chloride hexahydrate, neodymium nitrate hexahydrate, samarium chloride hexahydrate, europium chloride hexahydrate, and dysprosium nitrate pentahydrate were purchased from Aldrich Chemical Co. Inc. and were used as received. All other chemicals were of AR grade

Physical Measurements. Elemental analyses (carbon and hydrogen) were performed using a Perkin-Elmer 240C elemental analyzer. IR spectra were measured from KBr pellets on a Nicolet 520 FTIR spectrometer. Thermogravimetric analyses were carried out on a Mettler Toledo Star system.

Synthesis of $[Gd_2(suc)_3(H_2O)_2]\cdot 0.5H_2O$ (5). An aqueous solution (5 mL) of disodium succinate (0.162 g, 1 mmol) was added to an aqueous solution (10 mL) of gadolinium nitrate hexahydrate (0.301 g, 0.66 mmol) with constant stirring for 10 min. The resultant

(11) (a) Lauffer, R. B. *Chem. Rev.* **1987**, *87*, 901. (b) Aime, S.; Botta, M.; Fasano, M.; Terreno, E. *Chem. Soc. Rev.* **1998**, 27, 19. (c) Caravan, P.; Ellison, J. J.; McMurry, T. J.; Lauffer, R. B. *Chem. Rev.* **1999**, *99*, 2293. (d) Moonen, C. T. W.; van Zijl, P. C. M.; Frank, J. A.; Le Bihan, D.; Becker, E. D. *Science* **1990**, *250*, 53. (e) Kumar, K.; Chang, C. A.; Tweedle, M. F. *Inorg. Chem.* **1993**, *32*, 587. (f) Micskei, K.; Powell, D. H.; Helm, L.; Brucher, E.; Merbach, A. E. *Magn. Reson. Chem.* **1993**, *31*, 1011. (g) Gonzalez, G.; Powell, D. H.; Tissieres, V.; Merbach, A. E. *J. Phys. Chem.* **1994**, *98*, 53. (h) Powell, D. H.; Ni Dhubhghaill, O. M.; Pubanz, D.; Helm, L.; Lebedev, Y. S.; Schlaepfer, W.; Merbach, A. E. *J. Am. Chem. Soc.* **1996**, *118*, 9333. (i) Aime, S.; Botta, M.; Crich, S. G.; Giovenzana, G. B.; Jommi, G.; Pagliarin, R.; Sisti, M. *Inorg. Chem.* **1997**, *36*, 2992.

(12) (a) Molander, G. A. *Chem. Rev.* **1992**, *92*, 29. (b) Kobayashi, S.; Sugiura, M.; Kitagawa, H.; Lam, W. W. L. *Chem. Rev.* **2002**, *102*, 2227.

(13) (a) Shibasaki, M.; Yoshikawa, N. *Chem. Rev.* **2002**, *102*, 2187. (b) Gromada, J.; Carpentier, J. F.; Mortreux, A. *Coord. Chem. Rev.* **2004**, *248*, 397.

(14) Benelli, C.; Gatteschi, D. *Chem. Rev.* **2002**, *102*, 2369.

(15) Figuerola, A.; Diaz, C.; Ribas, J.; Tangoulis, V.; Sangregorio, C.; Gatteschi, D.; Maestro, M.; Mahia, J. *Inorg. Chem.* **2003**, *42*, 5274.

(16) Goodenough, J. B. *Magnetism and the Chemical Bond*; Interscience: New York, 1963.

(17) Kahn, O.; Briat, B. *J. Chem. Soc., Faraday Trans. 2* **1979**, *268*, 79.

(18) Hay, J. P.; Thibeault, J. C.; Hoffmann, R. *J. Am. Chem. Soc.* **1975**, *97*, 4884.

(19) (a) Costes, J.-P.; Dahan, F.; Nicodème, F. *Inorg. Chem.* **2001**, *40*, 5285. (b) Setyawati, I. A.; Liu, S.; Rettig, S. J.; Orvig, C. *Inorg. Chem.* **2000**, *39*, 496. (c) Dei, A.; Gatteschi, D.; Massa, C. A.; Pardi, S.; Poussereau, S.; Sorace, L. *Chem. Eur. J.* **2000**, *6*, 4580. (d) Guerriero, P.; Tamburini, S.; Vigato, P. A.; Benelli, C. *Inorg. Chim. Acta* **1991**, *189*, 19.

(20) (a) Panagiotopoulos, A.; Zafiropoulos, T. F.; Perlepes, S. P.; Bakalbassis, E.; Masson-Ramade, I.; Kahn, O.; Teris, A.; Raptopoulou, C. P. *Inorg. Chem.* **1995**, *34*, 4918 and references therein. (b) Hedinger, R.; Ghisletta, M.; Hegetschweiler, K.; Toth, E.; Merbach, A. E.; Sessoli, R.; Gatteschi, D.; Germlich, V. *Inorg. Chem.* **1998**, *37*, 6698. (c) Liu, S.; Gelmini, L.; Rettig, S. J.; Thompson, R. C.; Orvig, C. *J. Am. Chem. Soc.* **1992**, *114*, 6081. (d) Costes, J. P.; Dahan, F.; Dupuis, A.; Lagrave, S.; Laurent, J. P. *Inorg. Chem.* **1998**, *37*, 153. (e) Plass, W.; Fries, G. Z. *Z. Anorg. Allg. Chem.* **1997**, *623*, 1205. (f) Costes, J. P.; Dupuis, A.; Laurent, J. P. *Inorg. Chim. Acta* **1998**, *268*, 125.

(21) (a) Costes, J. P.; Clemente-Juan, J. M.; Dahan, F.; Nicodème, F.; Verelst, M. *Angew. Chem., Int. Ed.* **2002**, *41*, 323. (b) Hernández-Molina, M.; Ruiz-Pérez, C.; López, T.; Lloret, F.; Julve, M. *Inorg. Chem.* **2003**, *42*, 5456. (c) Hatscher, S. T.; Urland, W. *Angew. Chem., Int. Ed.* **2003**, *42*, 2862. (d) Baggio, R.; Calvo, R.; Garland, M. T.; Peña, O.; Perec, M.; Rizzi, A. *Inorg. Chem.* **2005**, *44*, 8979. (e) Roy, L. E.; Hughbanks, T. *J. Am. Chem. Soc.* **2006**, *128*, 568.

(22) Perles, J.; Iglesias, M.; Ruiz-Valero, C.; Snejko, N. *J. Mater. Chem.* **2004,** *14*, 2683.

(23) (a) Serpaggi, F.; Ferey, G. *Microporous Mesoporous Mater.* **1999**, *32*, 311. (b)Wang, C.-X.; Li, Z.-F. *Acta Crystallogr. Sect. E* **2005**, *61*, m2212. (c) Nika, W.; Pantenburg, I.; Meyer, G. *Acta Crystallogr., Sect. E* **2005**, *61*, m138. (d) Fleck, M. *Z. Kristallogr.-New Cryst. Struct.* **2002**, *217*, 569.

(24) (a) Guillou, N.; Livage, C.; van Beek, W.; Noguès, M.; Férey, G. *Angew. Chem., Int. Ed.* **2003**, *6*, 42. (b) Bowden, T. A.; Milton, H. L.; Slawin, A. M. Z.; Lightfoot, P. *J. Chem. Soc., Dalton Trans.* **2003**, 936. (c) Zheng, Y. Q.; Sun, J. *J. Solid State Chem.* **2003**, *178*, 288. (d) Forster, P. M.; Cheetham, A. *Angew. Chem., Int. Ed.* **2002**, *3*, 41.

Table 1. Crystal Data and Structure Refinement of **1**−**6**

	1	**2**	**3**	**4**	**5**	**6**
empirical formula	$C_{12}H_{17}Pr_2O_{14.5}$	$C_{12}H_{17}Nd_2O_{14.5}$	$C_{12}H_{17}Sm_2O_{14.5}$	$C_{12}H_{17}Eu_2O_{14.5}$	$C_{12}H_{17}Gd_2O_{14.5}$	$C_{12}H_{17}Dy_2O_{14.5}$
formula mass, g mol^{-1}	675.08	681.74	693.96	697.18	707.76	718.26
cryst system	monoclinic	monoclinic	monoclinic	monoclinic	monoclinic	monoclinic
space group	*I*2/a	*I*2/a	*I*2/a	*I*2/a	*I*2/a	*I*2/a
a, Å	14.015(3)	13.981(3)	13.919(3)	13.894(4)	13.865(4)	13.825(2)
b, Å	7.944(2)	7.910(2)	7.842(2)	7.809(2)	7.787(2)	7.7180(7)
c, Å	17.615(4)	17.561(4)	17.457(4)	17.421(6)	17.381(3)	17.321(3)
β, deg	102.05(2)	101.71(2)	101.15(3)	101.04(2)	101.02(2)	101.02(2)
Z	4	4	4	4	4	4
V, Å^3	1917.9(8)	1901.7(8)	1869.5(8)	1855.1(9)	1842.0(8)	1814.1(4)
D (calcd), g cm^{-3}	2.338	2.381	2.466	2.496	2.552	2.630
M (Mo Kα), mm^{-1}	5.093	5.473	6.295	6.775	7.214	8.251
F(000)	1292	1300	1316	1324	1332	1348
θ range, deg	2.96−31.09	2.83−28.28	2.86−30.57	2.87−31.05	2.88−30.57	3.04−30.59
no. of collcd data	12098	9268	11703	12453	10124	10735
no. of unique data	2903	2123	2279	2948	2799	2493
R_{int}	0.0228	0.0333	0.0434	0.0330	0.0681	0.0330
observed $I > 2\sigma(I)$	2519	1753	2275	2590	2376	2362
goodness of fit (F^2)	1.149	1.159	1.062	0.996	1.012	1.120
parameters	141	141	141	141	141	141
$R1$ ($I > 2\sigma(I)$)[a]	0.0304	0.0518	0.0291	0.0278	0.0300	0.0281
$wR2$[a]	0.0894	0.1526	0.0776	0.0714	0.0694	0.0790
$\Delta\rho$, e/Å^3	1.438, −0.663	2.776, −2.249	1.048, −1.746	1.329, −0.657	1.376, −1.167	1.303, −0.855

[a] $R1(F_o) = \sum||F_o| - |F_c||/\sum|F_o|$, $wR2(F_o^2) = [\sum w(F_o^2 - F_c^2)^2/\sum w(F_o^2)^2]^{1/2}$.

reaction mixture was transferred to a Teflon-lined steel vessel and was heated for 24 h at 175 °C. Colorless crystals (80% yield) suitable for X-ray analysis were obtained overnight by cooling the vessel to room temperature (∼27 °C). Found (%): C, 20.32; H, 2.42. Calcd for $C_{12}H_{17}Gd_2O_{14.5}$ (707.76) (%): C, 20.34; H, 2.40. The IR spectra exhibited the bands in the following regions: 3480−3025 (sbr); 1569 (vs); 1456 (vs); 1427 (vs); 1402 (vs); 1305 (m); 1215 (m); 1176 (m); 1002 (w); 908 (w); 651 (vw); 572 (vw) cm^{-1}.

Syntheses of $[Ln_2(suc)_3(H_2O)_2]\cdot 0.5H_2O$ [Ln = Pr (1), Nd (2), Sm (3), Eu (4), and Dy (6)]. All these complexes were synthesized as the procedure adopted for complex **5** using praseodymium chloride hexahydrate (0.236 g, 0.66 mmol), neodymium nitrate hexahydrate (0.292 g, 0.66 mmol), samarium chloride hexahydrate (0.243 g, 0.66 mmol), europium chloride hexahydrate (0.242 g, 0.66 mmol), and dysprosium nitrate pentahydrate (0.289 g, 0.66 mmol) for complexes **1**, **2**, **3**, **4**, and **6**, respectively. Suitable crystals of **1** (light green), **2** (violet), **3** (light yellow), **4**, and **6** (colorless) for X-ray diffraction analysis were obtained overnight on cooling the reaction vessels. The yields were 82%, 78%, 80%, 75%, and 70% for **1**, **2**, **3**, **4**, and **6**, respectively.

Elemental analyses are in good agreement with the calculated values. (**1**) Anal. Calcd for $C_{12}H_{17}Pr_2O_{14.5}$ (675.08) (%): C, 21.33; H, 2.51. Found (%): C, 21.35; H, 2.49. IR spectra: 3465−3035 (sbr); 1560 (vs); 1433 (vs); 1402 (vs); 1303 (m); 1215 (m); 1174 (w); 646 (vw) cm^{-1}. (**2**) Anal. Calcd for $C_{12}H_{17}Nd_2O_{14.5}$ (681.74) (%): C, 21.12; H, 2.49. Found (%): C, 21.15; H, 2.46. IR spectra: 3436−3190 (sbr); 1560 (vs); 1450 (vs); 1402 (vs); 1303 (m); 1215 (m); 1176 (m); 1001 (vw); 906 (vw); 648 (w); 570 (w) cm^{-1}. (**3**) Anal. Calcd for $C_{12}H_{17}Sm_2O_{14.5}$ (693.96) (%): C, 20.75; H, 2.44. Found (%): C, 20.73; H, 2.45. IR spectra: 3470−3040 (sbr); 1563 (vs); 1430 (vs); 1400 (vs); 1311 (m); 1219 (m); 1009 (w) cm^{-1}. (**4**) Anal. Calcd for $C_{12}H_{17}Eu_2O_{14.5}$ (697.18) (%): C, 20.65; H, 2.43. Found (%): 20.64; H, 2.44. IR spectra: 3460−3035 (sbr); 2928 (w); 2920 (w); 2863 (vw); 1567 (vs); 1567 (vs); 1427 (vs); 1403 (vs); 1305 (s); 1215 (s); 1176 (s); 1049 (m); 1001 (w); 974 (w); 907 (w); 877 (vw); 811 (w); 688 (m); 651 (m); 572 (w); 527 (vw) cm^{-1}. (**6**) Anal. Calcd for $C_{12}H_{17}Dy_2O_{14.5}$ (718.26) (%): C, 20.04; H, 2.36. Found (%): 20.05; H, 2.35. IR spectra: 3455−3050 (sbr); 2983 (w); 2920 (w); 1575 (vs); 1541 (vs); 1457 (s); 1428 (s); 1403 (s); 1305 (s); 1215 (m); 1177 (m); 1049 (w); 1002 (m); 954 (w); 910 (w); 878 (w); 691 (m); 654 (m); 572 (w); 530 (vw) cm^{-1}.

Crystallographic Data Collection and Refinement. Crystal data and details of data collections and refinements for the structures reported are summarized in Table 1. All the data collections were carried out at 293(3) K using Mo Kα radiation (λ = 0.71073 Å) on a Nonius DIP-1030H system. Cell refinement, indexing, and scaling of the data set were performed using programs Denzo and Scalepack.[25] According to Mighell[26] that "the maximum in utility of crystallographic data will be achieved if the experimentalist ... selects the type of cell centering (*I* or *C*) that leads to a conventional cell based on the shortest vectors in the ac plane (b-axis unique)", all structures were solved in space group *I*2/a. The structures were refined by the full-matrix least-squares method on the basis of F^2 with all observed reflections.[27] A residual present in all ΔF maps and located on 2-fold axis, was interpreted as a water oxygen with a population parameter of 0.25. However, it is not to be excluded that the amount of water might be slightly different in some compounds. All the calculations were performed using the WinGX System, Ver 1.64.05.[28]

Magnetic Measurements. The temperature dependence of the magnetic susceptibility of all the complexes was measured with a Cryogenic S600 SQUID magnetometer in the temperature range 3−290 K with an applied field of 0.099 T. Except for the Gd compound, the magnetic behavior of all the other complexes was reproduced in the framework of the classical crystal field model. The magnetic susceptibility, calculated in any case for a single 4f ion, was reproduced by applying the Van Vleck equation using only the energy levels originated by the splitting of the ground multiplet. The fittings of all the experimental data were performed

(25) Otwinowski, Z.; Minor, W. Processing of X-ray Diffraction Data Collected in Oscillation Mode. In *Macromolecular Crystallography*; Carter, C. W., Jr., Sweet, R. M., Eds.; Methods in Enzymology, Volume 276, Part A; Academic Press: 1997; pp 307−326.
(26) Mighell, A. D. *Acta Crystallogr., Sect. B* **2003**, *59*, 300. Monoclinic space group *C* 2/c, achieved through the 1 0 1, 0 1 0, −1 0 0 matrix, leads to a larger value (ca. 121°) for the β angle and to longer axes in the *ac* plane.
(27) Sheldrick, G. M. *SHELX97 Programs for Crystal Structure Analysis*, release 97-2; University of Göttingen: Göttingen, Germany, 1998.
(28) Farrugia, L. J. *J. Appl. Crystallogr.* **1999**, *32*, 837.

by minimizing the function

$$F = \frac{\sum_i [\chi_i^{obs} - \chi_i^{calc}]^2 T_i^2}{\sum_i [\chi_i^{obs} T_i]^2}$$

using the MINUIT program package.[29]

Computational Methods. All the calculations were performed in the framework of density functional theory (DFT)[30] with the NWChem program package.[31] The calculations were performed on trinuclear complexes appropriately chosen to model the relevant exchange pathways detected in the crystal structure as described in the text. The hybrid B3LYP functional[32] was used in all the calculations. The electron double-ζ basis set proposed by Dunning and Hay[33] was applied to all the atoms except for Gd that was treated using the Stuttgart relativistic small effective core potentials and the corresponding optimized basis set.[34] Population analysis based on natural atomic orbitals (NAO) and natural bond orbitals (NBO)[35] was performed using the NBO 5.0 program[36] implemented in NWChem. Calculations of the exchange coupling constant were performed using the broken symmetry formalism[37] as described in the text. All the calculations were performed using the "xfine" grid option to achieve an energy convergence of 10^{-8} hartree (2×10^{-3} cm^{-1}).

(29) James, F. *MINUIT*, version 94.1; CERN Program Library, CERN: Geneva, Switzerland.

(30) *Reviews of Modern Quantum Chemistry*; Sen, K. D., Ed.; World Scientific: Singapore, 2002; Vol. 1−2.

(31) (a) Aprà, E.; Windus, T. L.; Straatsma, T. P.; Bylaska, E. J.; de Jong, W.; Hirata, S.; Valiev, M.; Hackler, M.; Pollack, L.; Kowalski, K.; Harrison, R.; Dupuis, M.; Smith, D. M. A.; Nieplocha, J.; Tipparaju, V.; Krishnan, M.; Auer, A. A.; Brown, E.; Cisneros, G.; Fann, G.; Früchtl, H.; Garza, J.; Hirao, K.; Kendall, R.; Nichols, J.; Tsemekhman, K.; Wolinski, K.; Anchell, J.; Bernholdt, D.; Borowski, P.; Clark, T.; Clerc, D.; Dachsel, H.; Deegan, M.; Dyall, K.; Elwood, D.; Glendening, E.; Gutowski, M.; Hess, A.; Jaffe, J.; Johnson, B.; Ju, J.; Kobayashi, R.; Kutteh, R.; Lin, Z.; Littlefield, R.; Long, X.; Meng, B.; Nakajima, T.; Niu, S.; Rosing, M.; Sandrone, G.; Stave, M.; Taylor, H.; Thomas, G.; van Lenthe, J.; Wong, A.; Zhang, Z. *NWChem, A Computational Chemistry Package for Parallel Computers*, version 4.6; Pacific Northwest National Laboratory: Richland, WA, 2004. (b) Kendall, R. A.; Aprà, E.; Bernholdt, D. E.; Bylaska, E. J.; Dupuis, M.; Fann, G. I.; Harrison, R. J.; Ju, J.; Nichols, J. A.; Nieplocha, J.; Straatsma, T. P.; Windus, T. L.; Wong, A. T. High Performance Computational Chemistry: An Overview of NWChem a Distributed Parallel Application. *Comput. Phys. Commun.* **2000**, *128*, 260.

(32) Becke, A. D. *J. Chem. Phys.* **1993**, *98*, 5648.

(33) Dunning, T. H., Jr.; Hay, P. J. In *Methods of Electronic Structure Theory*; Schaefer, H. F., III, Ed.; Plenum Press: 1977; Vol. 2.

(34) Stuttgart RSC 1997 ECP was obtained from the Extensible Computational Chemistry Environment Basis Set Database, Version 02/25/04, as developed and distributed by the Molecular Science Computing Facility, Environmental and Molecular Sciences Laboratory which is part of the Pacific Northwest Laboratory, P.O. Box 999, Richland, WA 99352, and funded by the U.S. Department of Energy. The Pacific Northwest Laboratory is a multiprogram laboratory operated by Battelle Memorial Institute for the U.S. Department of Energy under contract DE-AC06-76RLO 1830.

(35) Reed, A. E.; Curtiss, L. A.; Weinhold, F. *Chem. Rev.* **1988**, *88*, 899.

(36) Glendening, E. D.; Badenhoop, J. K.; Reed, A. E.; Carpenter, J. E.; Bohmann, J. A.; Morales, C. M.; Weinhold, F. *NBO 5.0*; Theoretical Chemistry Institute, University of Wisconsin: Madison, WI, 2001; http://www.chem.wisc.edu/~nbo5.

(37) (a) Noodleman, L.; Norman, J. G., Jr. *J. Chem. Phys.* **1979**, *70*, 4903. (b) Noodleman, L. *J. Chem. Phys.* **1981**, *74*, 5737. (c) Noodleman, L.; Davidson, E. R. *Chem. Phys.* **1986**, *109*, 131. (d) Ciofini, I.; Daul, C. A.; Bencini, A. Modeling Molecular Magnetism. In *Recent Advances in DFT Methods*; Barone, V., Bencini, A., Fantucci, P., Eds.; World Scientific: Singapore, 2002; Vol. 1, Part III, p 106.

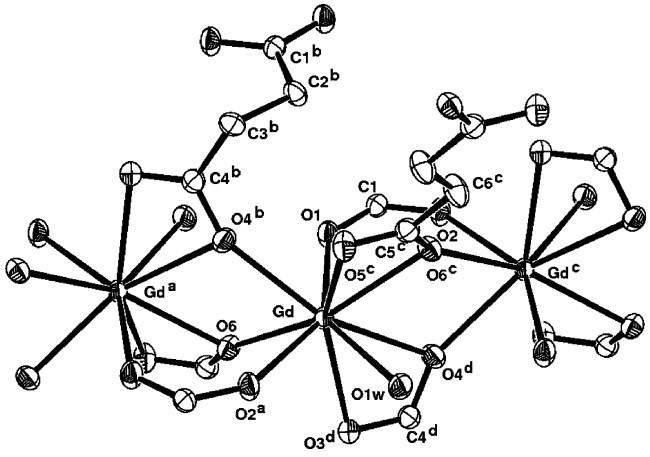

Figure 1. Detail of crystal packing in complex **5** showing the coordination sphere of three Gd(III) ions zigzag arranged along axis *b* and the conformations of succinate dianion (the same scheme applies also to other complexes, symmetry codes indicated in Table 2).

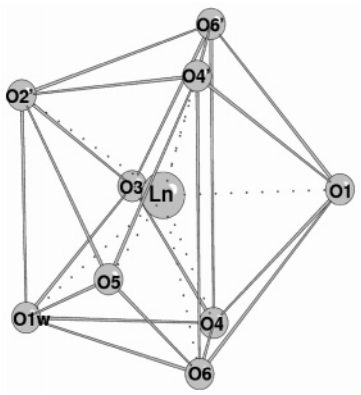

Figure 2. Coordination sphere of lanthanide forming a tricapped trigonal prism in all the structures reported.

Results and Discussion

Structure Descriptions. The structural determination of $[Ln_2(suc)_3(H_2O)_2]\cdot 0.5H_2O$ complexes [Ln = Pr (**1**), Nd (**2**), Sm (**3**), Eu (**4**), Gd (**5**), and Dy (**6**)] reveals that these are isomorphous and crystallize in monoclinic system, space group *I*2/a.

The X-ray diffraction analyses of complexes **1**−**6** reveal that lanthanide ions possess a nine-coordination geometry which comprises eight oxygen atoms from succinate dianions and one oxygen from a water molecule. In the frameworks, lanthanide polyhedra and dicarboxylate anions form layers which are interconnected by another organic anion to form a 3D network. Thus, two crystallographic independent dicarboxylates (Figure 1) are involved in the architecture assembly: one along the [001] and the other in the [100] direction in 1:2 ratio. Two adjacent Gd ions are connected by three carboxylate groups, of which one acts as a bridge in the usual $\eta^1{:}\eta^1{:}\mu_2$ mode while the other two serve as oxocarboxylate bridges in the less common $\eta^2{:}\eta^1{:}\mu_2$ fashion. Figure 1 shows a detail of the crystal structure of **5**. The coordination sphere results in a tricapped trigonal prism illustrated in Figure 2. The analysis of coordination bond lengths, reported in Table 2, indicates a range for Ln−O bond distances that varies in agreement with metal ionic

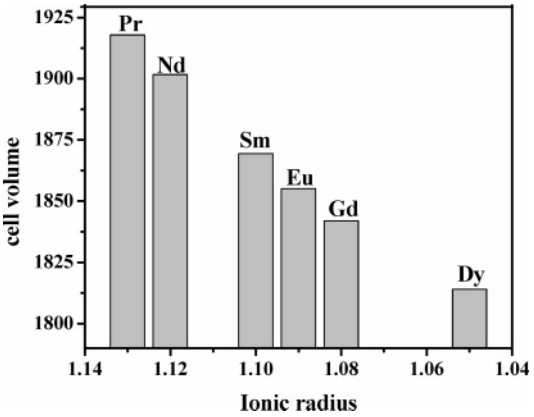

Figure 3. Plot of cell volume vs ionic radius.

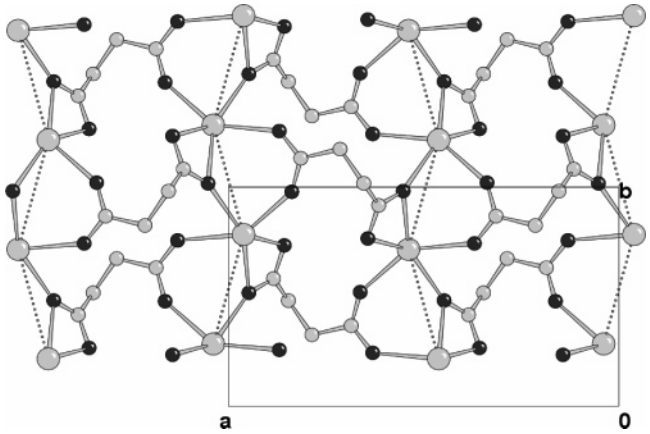

Figure 4. Corrugated layers in the crystallographic *ab* plane with lanthanide ions connected by C1−C4 succinate (coordinated water molecules not shown, dotted lines indicate Gd chain of Figure 1).

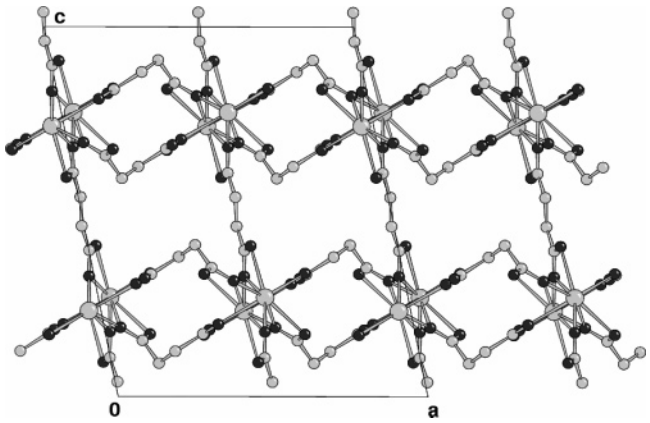

Figure 5. Crystal packing showing layers connected by centrosymmetric succinate fragments along axis *c*.

radius value. A plot of the cell volume versus +3 metal ionic radius shown in Figure 3 reveals a monotonically decreasing trend and reveals also that cell parameters follow a similar trend. The lanthanide polyhedra form a zigzag chain along axis *b*, with Ln(III) ions disposed at a distance from 4.02 to 4.14 Å and a Ln−Ln−Ln angle along the chain close to 147° for all the complexes (Table 2). The packing can be described as built up of $[Ln_2(H_2O)_2(suc)]_n$ layers parallel to 001 planes, containing the described polyhedra arrays, connected by succinate fragments that behave as bridging (carboxylate O(1)−C−O(2)) and chelating-bridging (O(3)−C−O(4)) toward four Ln(III) cations. A packing view down the [001] direction (Figure 4) evidences the described plane. These planes, separated by half axis *c*, are joined by another anion located on an inversion center that acts as chelating-bridging in a symmetric fashion (carboxylate O(5)−C−O(6)). The resulting three-dimensional framework (Figure 5) is responsible for the formation of small channels (∼5% of the cell volume[39]) containing disordered lattice water molecules. The two crystallographic independent succinate dianions have a gauche-staggered and an anti conformation, as indicated by the torsion angle values along the carbon skeleton of ca. 72° for the anion inserted in the *ab* plane and of 180.0° for the other.

The lattice water molecule, that resides on a 2-fold axis, was refined with a site occupancy of 0.25 in all the complexes (correspondent to 0.5 water molecule per $[Ln_2(suc)_3(H_2O)_2]$ unit), taking into account the height of the peak on the Fourier map. Isomorphous structures of Y, La, Pr,[22,23a] Gd,[38a] and Tb[38b] (solved in space group *C*2/*c*) were reported to contain a full lattice water molecule per formula unit. A careful analysis of displacement thermal parameters Ueq (Å^2) of the lattice water molecule in these compounds evidences values considerably higher (up to 7 times) in comparison

Table 2. Coordination Bond Lengths (Å), Significant Geometrical Parameters, and Torsion Angles (°) of the Succinate Dianion Connecting Lanthanide in the *ab* Plane of **1**−**6**

Coordination Bond Lengths and Geometrical Parameters						
	1 Pr	**2**	**3**	**4**	**5 Gd**	**6**
Ln−O(1)	2.504(3)	2.488(6)	2.461(4)	2.441(3)	2.427(3)	2.396(3)
Ln−O(2[a])	2.381(3)	2.378(5)	2.346(3)	2.325(2)	2.319(2)	2.288(2)
Ln−O(3[d])	2.558(3)	2.533(6)	2.506(4)	2.494(3)	2.483(3)	2.459(3)
Ln−O(4[b])	2.476(2)	2.461(5)	2.438(3)	2.434(2)	2.419(3)	2.394(2)
Ln−O(4[d])	2.605(3)	2.585(5)	2.558(3)	2.541(2)	2.536(3)	2.513(2)
Ln−O(5[c])	2.541(3)	2.527(6)	2.509(4)	2.495(3)	2.481(3)	2.461(3)
Ln−O(6)	2.474(3)	2.465(5)	2.438(3)	2.429(2)	2.427(3)	2.397(2)
Ln−O(6[c])	2.533(2)	2.515(5)	2.485(3)	2.474(2)	2.462(3)	2.439(2)
Ln−O(1w)	2.556(3)	2.544(5)	2.507(3)	2.485(2)	2.474(3)	2.442(2)
Ln−Ln[c]	4.1356(10)	4.1187(10)	4.0852(10)	4.0692(10)	4.0585(10)	4.0249(4)
Ln[a]−Ln−Ln[c]	147.66(1)	147.58(2)	147.40(2)	147.28(1)	147.21(1)	146.99(1)

Torsion Angles						
	1	**2**	**3**	**4**	**5**	**6**
C1/C2/C3/C4	72.6(4)	72.3(9)	72.7(5)	72.1(4)	71.9(4)	72.6(4)

[a] $-x+1, y-1/2, -z+1/2$. [b] $-x+3/2, -y+1/2, -z+1/2$. [c] $-x+1, y+1/2, -z+1/2$. [d] $x-1/2, -y+1, z$.

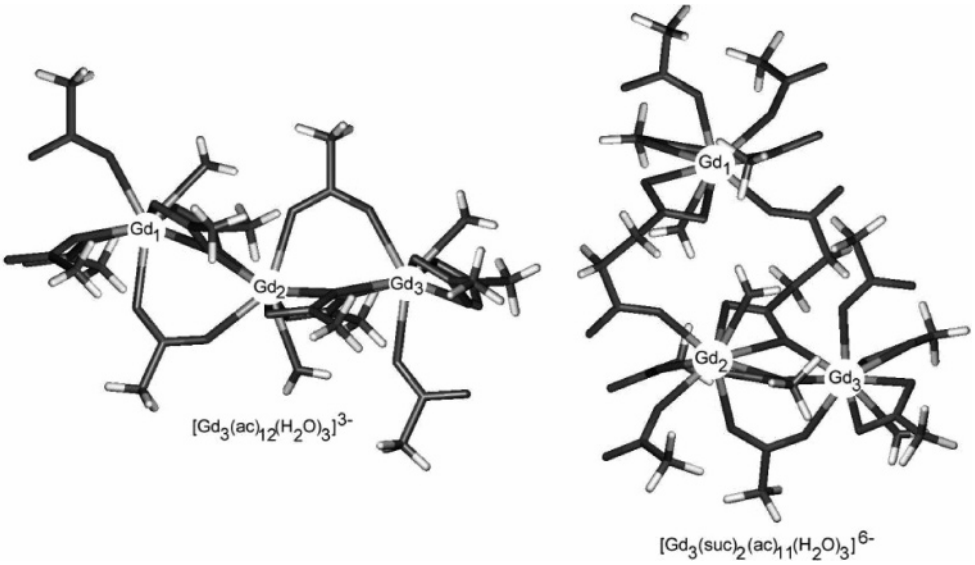

Figure 6. The trinuclear anionic model complexes used in the DFT calculations. The numbering of the Gd(III) ions corresponds to that used in the spin Hamiltonians (vide infra).

to those reported for coordinated oxygen atoms.[40] Although the lattice water molecule does not have an effective outcome on structural and magnetic properties of these complexes, we believe that the lattice water content should be considerably lower than that reported by other authors. However, since site occupancy and thermal factors are strongly correlated, it is not to be excluded that the amount of solvent might be slightly different in some of the compounds of the literature.

Gd[38a,c] and Eu[38b] succinate complexes containing no lattice water have also been reported. These 3D polymers crystallize in triclinic space group *P*1 and contain two crystallographic independent lanthanide ions (Ln1, Ln2) and three succinates. Both the metals possess a coordination sphere similar to complexes **1**−**6**, formed by eight oxygen atoms from carboxylate groups and one oxygen atom from the water molecule to furnish a tricapped trigonal prismatic geometry. However, the coordination modes of succinate ligands around Ln1 and Ln2 ions are slightly different, and the shortest intermetallic distance was measured to be 4.0763(7) Å (Eu−Eu) and 4.060 Å (mean value) for the Gd complexes, the latter value being close comparable to that of derivative **5** (Table 2).

Electronic Structure and Magnetic Properties of $[Gd_2(suc)_3(H_2O)_2]\cdot 0.5H_2O$ (5). The crystal structure of $[Gd_2(suc)_3(H_2O)_2]\cdot 0.5H_2O$ shows the presence of extended infinite extension along *b* and *c* axes leading to different exchange pathways. In the Gd(III) chains, developing along axis *b*, the metal ions are bridged by a syn−syn carboxylate and by two opposite oxygens from different CO_2^- groups that act as bischelating toward the nearby metal ion. This exchange pathway is represented in Figure 6 with the model, trinuclear cluster anion $[Gd_3(ac)_{12}(H_2O)_3]^{3-}$ (ac = acetate). This fragment was obtained from the crystal structure by substituting the $-CH_2CO_2$ residue of succinate by a H atom, leading to an acetate ion. These trinuclear units are linked along *c* by succinates as shown for the model cluster anion $[Gd_3(ac)_{11}(suc)_3(H_2O)_3]^{6-}$ in Figure 6. These two models were used to compute the magnetic exchange coupling constants to be compared with the experimental data. The calculation of the exchange coupling constants requires the knowledge of the energies of the spin multiplets arising from the vector coupling of the $S_i = 7/2$ ($i = 1-3$) spins of the Gd(III) anions. Since in the present case, $8^3 = 512$ states are possible, the computational task is enormous. Furthermore, the eigenstates of $\mathbf{S}^2$, where $\mathbf{S} = \mathbf{S}_1 + \mathbf{S}_2 + \mathbf{S}_3$ is the total spin operator, cannot be in general expressed as single Slater's determinant, and the accurate quantum chemical calculations of their energies would require a multiconfigurational-configuration interaction (MC−CI) approach that becomes practically impossible for systems of such chemical complexity. To circumvent this problem, a formalism was developed in recent years, and was widely applied, on the basis of the calculation of the spin state energies arising from those configurations where the metal ions have their maximum spin multiplicity, that is, ±7/2. These configurations are only 2^3 for a trinuclear system, and the correspondent energies computed at the DFT level are compared with those obtained from a spin Hamiltonian to obtain the exchange coupling constants.[37] In the present case, four independent spin configurations can be obtained by flipping one Gd(III) down from the high spin configuration and can be written as $|hs\rangle = |+++\rangle$, $|1\rangle = |-++\rangle$, $|2\rangle = |+-+\rangle$, $|3\rangle = |++-\rangle$, indicating with $|+\rangle$ the high spin state $S_i = 7/2$ on the *i*th Gd center. Four other configurations can be obtained by flipping the three spins in each set. These states are

(38) (a) Zhou, Y.-F.; Jiang, F.-L.; Yuan, D.-Q.; Wu, B.-L.; Hong, M.-C. *J. Mol. Struct.* **2005**, *743*, 21. (b) Cui, G.-H.; Li, J.-R.; Zhang, R.-H.; Bu, X.-H. *J. Mol. Struct.* **2005**, *740*, 187. (c) Zhang, H.-T.; Song, Y.; Li, Y.-X.; Zuo, J.-L.; Gao, S.; You, X.-Z. *Eur. J. Inorg. Chem.* **2005**, 766.

(39) Spek, A. L. PLATON package. *Acta Crystallogr., Sect A* **1990**, *C34*, 46.

(40) Data retrieved from original papers or through the Cambridge Data Base. Allen, F. H.; Kennard, O.; Taylor, R. *Acc. Chem. Res.* **1983**, *16*, 146.

degenerate with the previous ones in the absence of a magnetic field and are not useful for the calculation. While the $|hs\rangle$ configuration is an eigenstate of $\mathbf{S}^2$, the others are only eigenstates of $\mathbf{S}_z$. We will call the eigenstates of $\mathbf{S}^2$ pure spin states. The energies of the above four states can be expressed using the spin Hamiltonian[41] $H_S = J_{12}S_1 \cdot S_2 + J_{13}S_1 \cdot S_3 + J_{23}S_2 \cdot S_3$ as

$$E(hs) = E_0 + \frac{49}{4}[J_{12} + J_{13} + J_{23}] \quad (1)$$

$$E(1) = E_0 + \frac{49}{4}[-J_{12} - J_{13} + J_{23}] \quad (2)$$

$$E(2) = E_0 + \frac{49}{4}[-J_{12} + J_{13} - J_{23}] \quad (3)$$

$$E(3) = E_0 + \frac{49}{4}[J_{12} - J_{13} - J_{23}] \quad (4)$$

where E_0 is a spin independent term containing the average values of the kinetic energy of the electrons, the electron−nucleus repulsion, and so on. It is generally assumed that this term does not depend on the spin distribution and therefore cancels out while taking into account the energy differences among eqs 1−4. This is surely true when the covalency of the metal−ligand bonds is small, like in Gd complexes, but the assumption can be no longer valid in more general cases.[42] Indeed, the above formalism requires that the unpaired electrons are well localized onto the different metal ions, but this localization can change according to the spin distributions and can cause the spin independent term to change from one configuration to another. In the present case, the electron localization is almost perfect and independent from the spin configuration as can be seen from the population analysis as discussed later. Taking the differences Δ_{1j} between eqs 1 and 2−4, the working eqs 5−7 for the calculations of the J_{ij}'s are obtained:

$$\Delta_{12} = \frac{49}{2}[J_{12} + J_{13}] \quad (5)$$

$$\Delta_{13} = \frac{49}{2}[J_{12} + J_{23}] \quad (6)$$

$$\Delta_{14} = \frac{49}{2}[J_{13} + J_{23}] \quad (7)$$

The results of the DFT calculations on the complex anions $[Gd_3(ac)_{12}(H_2O)_3]^{3-}$ and $[Gd_3(ac)_{11}(suc)_3(H_2O)_3]^{6-}$ are reported in Table 3. The computed expectation values of $\mathbf{S}^2$ for all the unrestricted open shell determinants agree well with the values expected for weakly interacting magnetic orbitals (shown in parentheses).[43,44] The computed J_{ij} values show that a weak ferromagnetic coupling is operative between centers bridged by carboxylate groups with an average coupling constant $J_{av} = -0.041$ cm^{-1}, that agrees well with the experimental findings (vide supra). The exchange interaction through the succinate groups (J_{12} and J_{13} of $[Gd_3(ac)_{11}(suc)_3(H_2O)_3]^{6-}$) is computed to be zero, showing that these intrachain interactions should be negligible.

Table 3. Computed Energies and J_{ij} Values (cm^{-1})[a] for $[Gd_3(ac)_{12}(H_2O)_3]^{3-}$ and $[Gd_3(ac)_{11}(suc)_3(H_2O)_3]^{6-}$

determinant	$\langle \mathbf{S}^2 \rangle$[b]	$\Delta E = E(hs) - E(n)$ (cm^{-1})
	$[Gd_3(ac)_{12}(H_2O)_3]^{3-}$	
$\|hs\rangle = \|+++\rangle$	120.77 (120.75)	0.00
$\|1\rangle = \|-++\rangle$	22.77 (22.75)	−2.00
$\|2\rangle = \|+-+\rangle$	22.77 (22.75)	−0.96
$\|3\rangle = \|++-\rangle$	22.77 (22.75)	−0.66
$J_{12} = -0.04\ 7$	$J_{13} = 0.00\ 8$	$J_{23} = -0.03\ 5$
	$[Gd_3(ac)_{11}(suc)_3(H_2O)_3]^{6-}$	
$\|hs\rangle = \|+++\rangle$	120.77 (120.75)	0.00
$\|1\rangle = \|-++\rangle$	22.77 (22.75)	−0.78
$\|2\rangle = \|+-+\rangle$	22.77 (22.75)	0.01
$\|3\rangle = \|++-\rangle$	22.77 (22.75)	−0.80
$J_{12} = 0.00\ 1$	$J_{13} = 0.00\ 0$	$J_{23} = -0.03\ 2$

[a] The last digit is affected by the precision of the SCF convergence. [b] In parentheses the expected values for orthogonal α/β orbitals are reported.

Despite the wide successes of DFT in computing the sign and the relative order of magnitude of the magnetic exchange coupling constants,[37] no information can be directly obtained from the calculation about the detailed mechanisms (i.e., localized atomic orbitals involved) governing the exchange pathways; ab initio CAS-CI techniques are the best techniques to achieve this information.[45] However, the electronic population of the Gd ions in the molecules gives some hints in this direction. In all the calculations, the Mulliken spin population (spin density, e/Å^3) on the Gd ions is close to $|7.00 \div 7.01|$ and is <0.00 on all the other atoms, indicating that all the unpaired spins are well localized onto the metal centers. The spin distribution computed for $[Gd_3(ac)_{12}(H_2O)_3]^{3-}$ in the $|hs\rangle$ state shows that a spin delocalization mechanism is operative that spreads the electron spin about oxygens and carbons (same sign of the bonded Gd), except for the methyl carbon atoms where a small negative spin density is computed (spin polarization mechanism). The natural population analysis (NPA) agrees with the Mulliken one: the spin populations on Gd atoms are $6.98 \div 6.99$, the spin densities on the bridging oxygens of acetate are $0.001 \div 0.003$, and on the water oxygens they are 0.001. The NPA charges on Gd are 2.59 corresponding to an electron configuration $\{[Kr]\ 6s^{0.22}\ 4f^{7.03}\ 5d^{0.15}\ 6p^{0.01}\}$. This population shows a significant contribution of both 6s and 5d orbitals that can contribute to ferromagnetic pathways, being orthogonal to the 4f magnetic electrons. Similar calculations have been reported in a recent paper.[21e] The exchange coupling constant J_{23} (−0.03 cm^{-1}), computed for $[Gd_3(ac)_{11}(suc)_3(H_2O)_3]^{6-}$,

(41) With this spin Hamiltonian, a negative sign of J_{ij} indicates a ferromagnetic coupling.

(42) Bencini, A.; Totti, F. Manuscript in preparation.

(43) For an unrestricted open shell determinant, the expectation value of $\mathbf{S}^2$ is given by $\langle S^2 \rangle = (N_\alpha - N_\beta/2)^2 + (N_\alpha + N_\beta/2) - \sum_{ij}|S_{ij}^{\alpha\beta}|^2$ where $S_{ij}^{\alpha\beta}$ is the overlap integral between α and β orbitals. When the last term is zero, this corresponds to a complete localization of the magnetic electron and the limit value of a restricted open shell system is reached. In this situation, the mapping of the unrestricted wave function with the spin Hamiltonian is expected to hold.

(44) (a) Szabo, A.; Ostlund, N. S. *Modern Quantum Chemistry*; Dover Publications: New York, 1996. (b) O'Brien, T. A.; Davidson, E. R. *Int. J. Quantum Chem.* **2003**, *92*, 294.

(45) Cabrero, J.; Calzado, C. J.; Maynau, D.; Caballol, R.; Malrieu, J. P. *J. Phys. Chem. A* **2002**, *106*, 8146.

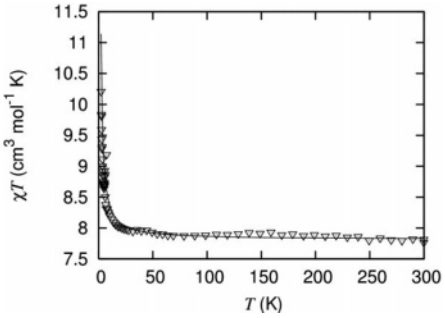

Figure 7. Temperature dependence of the magnetic susceptibility of **5**. The solid line represents the best fit curve obtained by the Curie−Weiss law (vide infra).

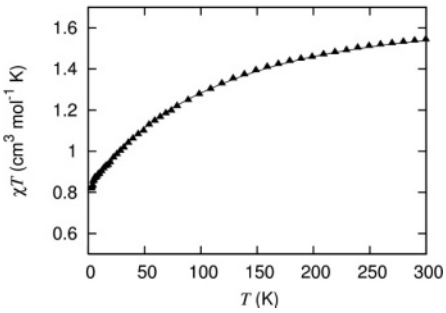

Figure 8. Temperature dependence of the magnetic susceptibility of **2**. The solid line represents the best fit curve obtained as described in the text.

is in good agreement with that obtained for $[Gd_3(ac)_{12}(H_2O)_3]^{3-}$ and shows that the succinate dianions are not effective in transmitting the exchange interaction.

The room-temperature magnetic susceptibility of $[Gd_2(suc)_3(H_2O)_2]\cdot 0.5H_2O$ agrees with the values usually found for isolated Gd(III) ion ($\chi^*T = 7.82$ emu mol^{-1} K^{-1} × Gd ion) and increases up to 10.94 emu mol^{-1} K^{-1} as shown in Figure 7. This behavior suggests the presence of some ferromagnetic interaction and the analysis of these data, by using the Curie−Weiss equation, confirms the presence of an overall ferromagnetic interaction. The best fit parameters are $C = 7.58(2)$ emu mol^{-1} K^{-1} and $\Theta = 0.593(4)$ K. The Weiss constant is related to the exchange coupling constant between adjacent centers by $\Theta = -zJS(S+1)/3k$, assuming an exchange coupling constant J equal for all the z nearest neighbor centers, we get $J = -0.039$ cm^{-1} with $z = 2$. This value agrees well with the values of J_{12} and J_{23} computed for the model trimer $[Gd_3(ac)_{12}(H_2O)_3]^{3-}$. We computed for $[Gd_3(ac)_{11}(suc)_3(H_2O)_3]^{6-}$ and observed that the value $z = 2$ is consistent with the negligible contribution of the exchange pathways (J_{12} and J_{13}). The magnetic data of $[Gd_2(suc)_3(H_2O)_2]\cdot 0.5H_2O$ can also be fitted with other models, as for example, by using the Fisher approach[46] for a chain of classical spins. The best fit is achieved with the parameters $g_{Gd} = 1.99(1)$ and $J = -0.019(5)$ cm^{-1}. In any case, a ferromagnetic interaction is operative between the Gd ions.

Magnetic Properties of (1), (2), (3), and (6). As these systems contain rare-earth ions with an orbitally degenerate ground state, it was not possible to use the previously described models to interpret their magnetic properties, and DFT calculations were not performed on these systems. The first attempt to reproduce the temperature dependence was made considering the 4f ions as isolated ones, and the magnetic properties were calculated in the framework of a classical crystal field (CF) approach. In all the calculations, an overall C_{2v} symmetry was assumed in order to reduce the CF parameters.

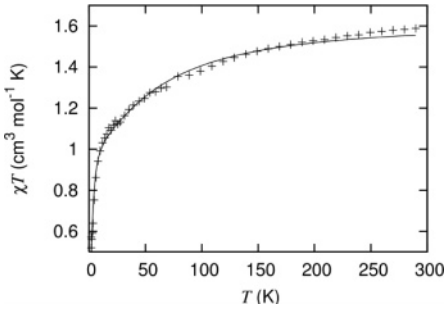

Figure 9. Temperature dependence of the magnetic susceptibility of **1**. The solid line represents the best fit curve obtained as described in the text.

Table 4. Best Fit Parameters (cm^{-1}) Used in the Crystal Field Calculations of **1**, **2,** and **3**

	B_2^0	B_2^2	B_4^0	B_4^2	B_4^4	B_6^0	B_6^2	B_6^4	B_6^6
1	123.6	772.3	−90.5	254.7	114.2	−21.2	97.9	158.1	−130.5
2	492.8	166.5	139.1	172.3	226.2	−9.1	101.9	101.3	999.2
3	334.6	810.8	43.4	232.1	−25.4	10.6	−167.9	22.6	50.8

The temperature dependence of the magnetic susceptibility of the Nd derivative (**2**) down to 20 K was nicely reproduced (Figure 8) with a ground Kramers doublet formed by a mixture of the $|\pm 7/2\rangle$ and $|\pm 5/2\rangle$ states with the next excited doublet at 83 cm^{-1}. Below this temperature, the experimental values are lower than the calculated ones (Figure 8). We therefore attempted to reproduce this behavior by assuming the presence of some kind of magnetic interaction. According to the calculated CF splitting of the $^4I_{9/2}$ ground multiplet of Nd(III), only the ground doublet is thermally populated below 25 K. Therefore, we tried to reproduce the magnetic behavior below this temperature with a molecular field (MF) approach using the effective g_{eff} value of 2.67 obtained from the composition of the ground Kramers doublet. The magnetic susceptibility was calculated[47] as $\chi_{MF} = \chi/(1 - nzJ\chi/0.2607295g_{eff}^2)$ where χ is the magnetic susceptibility calculated with the fixed CF parameters. The fitting procedure nicely reproduces the experimental pattern because of the presence of a weak antiferromagnetic interaction $nzJ = 0.11$ cm^{-1} (Figure 8). The CF parameters used in the calculations for all the complexes are collected in Table 4.

The temperature dependence of the magnetic susceptibility for the Pr (**1**) and Sm (**3**) derivatives was reproduced with the CF parameters shown in Table 4. For both the complexes, the experimental data were nicely reproduced in the whole temperature range (Figures 9 and 10) without introducing any kind of magnetic interaction. Probably, dipolar magnetic

(46) Bonner, J. C. In *Magneto-Structural Correlations in Exchange Coupled Systems*; Willett, R. D., Gatteschi, D., Kahn, O., Eds.; NATO Asi Series, C; D. Reidel Pub. Co.: 1985; Vol. 140, p 157.

(47) O'Connor, C. J. *Prog. Inorg. Chem.* **1982**, *29*, 203.

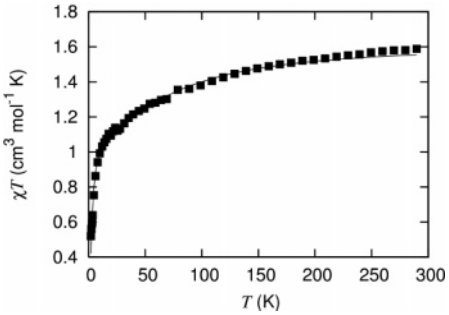

Figure 10. Temperature dependence of the magnetic susceptibility of **3**. The solid line represents the best fit curve obtained as described in the text.

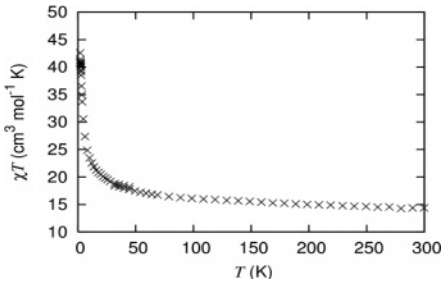

Figure 11. Temperature dependence of the magnetic susceptibility of **6**.

interactions are still active, but their effects are less effective than crystal field ones that overcome any possible magnetic interaction.

The temperature dependence of the magnetic susceptibility of the Dy derivative[48] is shown in Figure 11. The continuous increase of the χT values on lowering the temperature indicates the presence of ferromagnetic interaction as expected for Dy(III) ions,[49] and it is strong enough to overcome the CF effects that in general produce a decrease in the χT versus T curve. A simple calculation for dipolar interaction on the basis of Dy−Dy pairs on the basis of the observed Dy−Dy mean intermetallic distance was not able to produce the measured behavior. AC measurements of the magnetic properties at low temperature are in progress to clarify the roles as either crystal field or intermolecular effects. Actually, the low-temperature χT values are compatible in the presence of magnetic interactions extended to a lattice level whose interpretation demands the use of a quite complex model rather different from that used in this Paper.

(48) Caneschi, A. Preliminary results from Dipartimento di Chimica, Università di Firenze. Private communication.
(49) Ishikawa, N.; Iino, T.; Kaizu, Y. *J. Am. Chem. Soc.* **2002**, *124*, 11440.

Thermal Analyses. Thermogravimetric analysis reveals that all the complexes upon heating lose 0.5 molecule of lattice water and 2 molecules of coordinated water in one step (Figures 2S−4S). The initial temperature (T_i) for dehydration does not show any dependence on the atomic number. The T_i corroborates the involvement of lattice water in H-bonding. The dehydrated networks collapse at ∼300 °C.

Conclusions

Complexes of general formula $[Ln^{III}_2(suc)_3(H_2O)_2]\cdot 0.5H_2O$ [suc = succinate dianion, Ln = Pr, Nd, Sm, Eu, Gd, and Dy] have been synthesized and structurally characterized through X-ray diffraction analysis revealing a three-dimensional network of Ln(III) ions and carboxylate dianions. The magnetic properties of the Pr, Nd, Sm, Gd, and Dy derivatives have been measured. DFT calculations of the electronic structure of the Gd(III) derivative show that exchange interactions are effective only between ions connected by bridging carboxylates. These findings give the basis for the interpretation of the magnetic properties of the complex. The exchange interaction between Gd(III) ions was computed to be ferromagnetic which is in nice agreement with the experimental findings. Antiferromagnetic interactions have been found to be operative between Nd(III) ions, while they are negligible in the Pr(III) and Sm(III) complexes. The magnetic properties of the Dy(III) derivative showed a net increase of the effective magnetic moment on decreasing the temperature, and the origin of this potentially interesting magnetic behavior is the topic of deeper investigations.

Acknowledgment. Authors thank Council of Scientific and Industrial Research, New Delhi and MAGMANet [contract: NMP3-CT-2005-515767] for financial support. Thanks are expressed to Prof. Andrea Caneschi (Università di Firenze) for collecting the magnetic data.

Supporting Information Available: X-ray crystallographic data, in CIF format, and other crystallographic information, figures showing the coordination mode and the conformation of the two crystallographic independent succinate dianions, and TG curves of complexes **1**, **4**, and **6** are provided as Supporting Information. This material is available free of charge via the Internet at http://pubs.acs.org

IC060807D